Microchimica Acta (2018) 185: 366
https://doi.org/10.1007/s00604-018-2889-0

ORIGINAL PAPER

A fluorometric clenbuterol immunoassay based on the use of organic/inorganic hybrid nanoflowers modified with gold nanoclusters and artificial antigen

Tao Peng[1] · Jianyi Wang[1] · Sijun Zhao[2] · Sanlei Xie[1] · Kai Yao[1] · Pimiao Zheng[1] · Sihan Wang[1] · Yuebin Ke[3] · Haiyang Jiang[1]

Received: 12 April 2018 / Accepted: 26 June 2018 / Published online: 7 July 2018

Abstract

Organic/inorganic hybrid nanoflowers were synthesized from calcium phosphate and protein modified fluorescent gold nanoclusters and antigens. These nanoflowers are shown to be well suited labels for bioassay because they fulfill the functions of biological recognition and signal output. A fluorometric immunoassay was developed that was combined with immunomagnetic separation. In the detection system, the red fluorescence of the supernatant (measured at excitation/emission wavelengths of 360/640 nm) is found to be proportional to the clenbuterol (Clen) concentration after two immunomagnetic separations. The assay has a linear response in the 0.5 μg L^{-1} to 40 μg L^{-1} Clen concentration range, and 0.167 μg L^{-1} limit of detection. This makes it well suited for food safety monitoring. The average recoveries from spiked samples range from 92.7 to 109.1% (intra-assay) and 101.2 to 125.7% (inter-assay) with relative standard deviations of <11.6%. Spiked swine urine samples were analyzed by this method, and the results correlated well with data obtained by LC-MS/MS.

Keywords Fluorescent hybrid nanoflowers; calcium phosphate · BSA-AuNCs · Biomolecules immobilization · Biotin-streptavidin system · Immunomagnetic separations · Bioassay · Veterinary drug residues · Swine urine · Food safety monitoring

Introduction

The consumption of animal-derived foods has been increasing rapidly, thereby promoting the development of livestock breeding and the application of veterinary drugs. However, the abuse and misuse of veterinary drugs may accumulate in animal bodies, causing substantial damage to human health through the food chain if the residues are above certain levels [1]. Nowadays, many efforts have been exerted to develop a wide variety of analytical methods for the determination of veterinary drug residues to ensure food quality and safety [2]. Immunoreaction-based techniques are very attractive for the rapid detection of veterinary drug residues because of their simplicity and low cost, for instance, enzyme linked immunosorbent assay (ELISA), lateral flow immunoassay, and so forth. To obtain more sensitive detections, many fluorescent nanomaterials, such as quantum dots [3] and fluorescent microspheres [4], have been used as labels for the development of fluorometric immunoassays. Nobel metal nanoclusters (NMNCs), including gold, silver, and platinum nanoclusters, exhibit superior optical and physicochemical properties [5–7]. Thus, NMNCs have attracted tremendous research interests as a new type of fluorescent nanomaterials because of their good biocompatibility, low toxicity, and excellent

Electronic supplementary material The online version of this article (https://doi.org/10.1007/s00604-018-2889-0) contains supplementary material, which is available to authorized users.

✉ Haiyang Jiang
haiyang@cau.edu.cn

[1] Beijing Advanced Innovation Center for Food Nutrition and Human Health, College of Veterinary Medicine, China Agricultural University, Beijing Key Laboratory of Detection Technology for Animal-Derived Food Safety, Beijing Laboratory for Food Quality and Safety, Beijing 100193, People's Republic of China

[2] China Animal Health and Epidemiology Center, Qingdao 266032, People's Republic of China

[3] Shenzhen Center for Disease Control and Prevention, Shenzhen 518055, People's Republic of China

stability [8]. Cytidine [9], bovine serum albumin (BSA) [10], DNA [11], and methionine [12] have been applied to synthesize NMNCs. BSA-capped fluorescent gold nanoclusters (BSA-AuNCs) are the most common and have been applied to many areas [13–17]. However, few reports regarding BSA-AuNCs employed as labels in fluorometric immunoassays for the detection of veterinary drug residues are published.

Universally, the fluorescent nanomaterial-biomolecule conjugates are the most critical reagent in fluorometric immunoassay. Covalent coupling methods, including glutaraldehyde and active ester methods, are usually applied to prepare the conjugates. However, the preparation methods are relatively complicated and inefficient and often result in inevitable function sacrifice of nanomaterials and biomolecules because of organic solvent and chemical reactions [18, 19]. Thus, removing the bottleneck is important to obtain the conjugates that retain high activity. The immobilization of biomolecules has been approached by the synthesis of organic/inorganic hybrid nanoflowers, which can avoid the use of organic solvent [20]. Organic/inorganic hybrid nanoflowers, which are simply fabricated by adding protein to metal ion solution, are reported by Zare et al. in 2012 [21]. The preparation of organic/inorganic hybrid nanoflowers include immobilization, conjugation, crosslinking, and self-assembly, which does not contain any organic solvent and complex chemical reactions [22, 23]. Thus, the organic/inorganic hybrid nanoflowers have gained substantial research attention as a novel host platform for immobilizing biomolecules [20]. Wei et al. [18] constructed and applied antibody-enzyme-inorganic hybrid nanoflowers as a novel signal label in an ELISA for signal amplification ultrasensitive determination of *Escherichia coli* O157:H7. Ye et al. [19] presented a green method for the synthesis of concanavalin A-invertase-$CaHPO_4$ hybrid nanoflowers for point-of-care bioassays. Streptavidin-horseradish peroxidase hybrid nanoflowers were prepared and used for the ultrasensitive detection of alpha-fetoprotein [24]. Inspired by those works, the nanoflowers become fluorescent by loading BSA-AuNCs. Thus, fluorescent hybrid nanoflowers with BSA-AuNCs and artificial antigen have been synthesized. Calcium phosphate acted as the inorganic component, while the nanoflowers integrate the functions of biological recognition and fluorescence signal output.

In this work, Clenbuterol (Clen) was selected as the model target detected by the fluorometric immunoassay based on fluorescent hybrid nanoflowers. Clen, which belongs to the family of β_2–agonists, is illegally used as growth promoter because high dosages of Clen can promote animal muscular mass development and decrease fat accumulation, resulting in a higher muscle-to-fat ratio [25–27]. Food safety incidents regarding Clen residues have drawn attention worldwide; the accumulative residues of Clen in animal products are very harmful and can cause death in severe cases [28, 29]. Thus, Clen has been banned for use as a veterinary drug or food additive in China, the United States, and the European Union [30, 31]. However, the illicit use of Clen has not been prohibited absolutely because of its enormous economic benefits. The gas chromatography/mass spectrometry (GC/MS) or liquid chromatography–tandem mass spectrometry (LC-MS/MS) methods are using to monitor clenbuterol in animal farming by the Chinese government, which exhibit good sensitivity, selectivity and accuracy, but these methods demand time-consuming and complicated sample pretreatment process, and professional operations [27, 32]. In this system, immunomagnetic separation technique with the functions of immediate and efficient isolation and concentration of target in samples was induced to reduce the matrix effects [33]. Scheme 1 shows that the anti-Clen antibody is oriented and immobilized on the magnetic nanoparticles through biotin-streptavidin system, which acts as capture probes to enrich and separate Clen in swine urine samples. The nanoflowers were combined with the capture probes after the enrichment of Clen. Finally, the fluorescence intensity of the supernatant after immuonomagnetic separation, which would be proportional to the concentration of Clen in samples, was measured. Overall, the fluorescent-hybrid nanoflowers possess high biorecognition and favorable fluorescence signal with immunomagnetic separation. The method provides an optional approach for screening Clen residues.

Experimental section

Chemicals

BSA, and chloroauric acid ($HAuCl_4 \cdot 3H_2O$) were obtained from Sigma–Aldrich Chemical Corporation (St. Louis, USA, https://www.sigmaaldrich.com). Sulfo-NHS-biotin was purchased from Aladdin Reagent Co. (Shanghai, China, http://www.aladdin-e.com). Streptavidin magnetic particles (SA-MNPs) were obtained from Roche Diagnostics GmbH (Mannheim, Germany, https://www.roche.com). Dimethylsulphoxide (DMSO), sodium bicarbonate ($NaHCO_3$), calcium chloride ($CaCl_2$), and sodium hydroxide (NaOH) were purchased from Sinopharm Chemical Reagent Beijing Co., Ltd. (Beijing, China http://www.sinoreagent.com). Clen, salbutamol (Sal), ractopamine (Rac), zilpaterol (Zil), Phenylethanolamine A (PheA) were obtained from National Institutes for Food and Drug Control (Beijing, China, http://www.nicpbp.org.cn). Artificial antigen of Clen (Clen-BSA) and monoclonal antibody against Clen (Clen-mAb) were provided by Beijing WDWK Biotechnology Co. (Beijing, China, http://www.wdwkbio.com). All solvents and other chemicals were of analytical reagent grade.

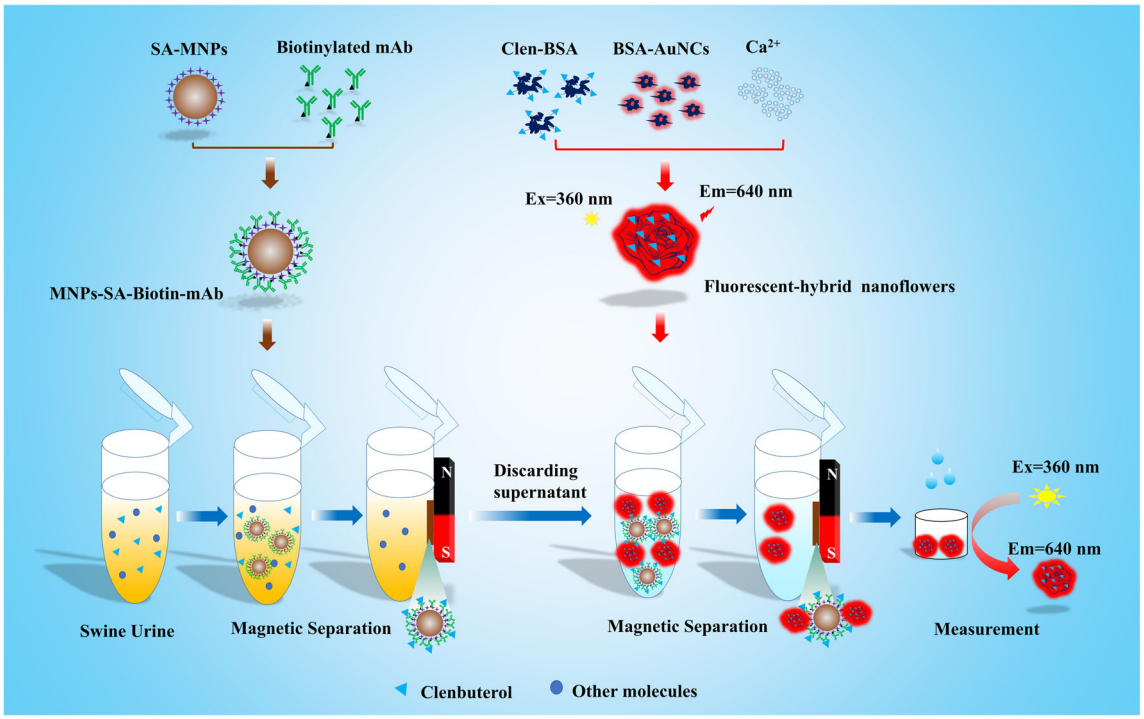

Scheme 1 Schematic of the fluorometric immunoassay based on the use of fluorescent hybrid nanoflowers and immunomagnetic separation

Apparatus

Dialysis bag (3500 Da) was purchased from Beijing Solarbio Science & Technology Co., Ltd. (Beijing, China, http://www.solarbio.com). The Nano Drop ND-2000 spectrophotometer was supplied by Thermo Fisher Scientific Inc. (Hong Kong, China https://www.thermofisher.com/cn). The multifunctional microplate reader SpectraMax M5 was purchased from Molecular Devices Co., Ltd. (Sunnyvale, CA, USA https://www.moleculardevices.com). Ultrapure water was purified using Milli-Q system from Millipore Corp. (Bedford, MA, USA http://www.merckmillipore.com). Scanning electron microscope (SEM) measurements were conducted on MERLIN Compact (Carl Zeiss, Germany), whereas transmission electron microscopy (TEM) measurements were conducted on a JEM100CXII transmission electron microscope (JEOL, Japan).

Fabrication of fluorescent-hybrid nanoflowers with BSA-AuNCs and Clen-BSA

Firstly, the BSA-AuNCs were synthesized with minor modification according to the previous work [34], and the process of synthesis is described detailedly in the Electronic Supporting Material (ESM). Secondly, 150 μL of aqueous $CaCl_2$ solution (120 mM) was added to 5 mL of phosphate buffered saline (PBS, 3 mM, pH 7.4) that contains 36 μg mL^{-1} of Clen-BSA and 152 μg mL^{-1} of BSA-AuNCs, followed by the aging reaction at room temperature for 18 h. The nanoflowers were obtained after washing with ultrapure water twice and resuspended using 5 mL of 2% BSA solution (*w/v*).

Preparation of biotinylated Clen-mAb

In a typical experiment, one milligram of Sulfo-NHS-Biotin was dissolved with 1 mL of DMSO. A total of 40 μL of Clen-mAb was dispersed in 1460 μL of $NaHCO_3$ solution (0.1 M), and 100 μL of sulfo-NHS-biotin solution (1 mg mL^{-1}) was added. After reacting for 2 h, the mixture was dialyzed using a dialysis bag (3500 Da) in phosphate buffered saline (0.01 M, pH 7.0) for 48 h to purify the biotinylated Clen-mAb, and stored at 4 °C until ready for use.

Preparation of immunomagnetic nanoparticles

Immunomagnetic nanoparticles (MNPs-SA-Biotin-mAb) are prepared as follows: Biotinylated Clen-mAb was typically added to the solution of SA-MNPs and reacted for approximately 30 min with gentle shaking at 37 °C. The MNPs-SA-Biotin-mAb was separated using magnetic force, washed twice with PBS buffer, and then resuspended in 1 mL of phosphate buffered saline (0.01 M, pH 7.0).

Protocol for the fluorometric immunoassay for Clen detection

A total of 500 μL of swine urine samples were mixed with 20 μL of MNPs-SA-Biotin-mAb and incubated at 37 °C for

30 min. After being separated by using a magnetic device and washed twice with PBS (phosphate buffered saline) that contains 0.05% Tween-20 (*v/v*), 500 μL of hybrid nanoflower solution that contains 2% BSA (*w/v*) was added. After reacting with continuous stirring for 15 min at 37 °C, the conjugation of nanoflowers and MNPs-SA-Biotin-mAb were separated by magnetic force. Subsequently, 100 μL of supernatant was subjected to fluorescence measurement with excitation at 360 nm and emission at 640 nm. Other structural analogues were spiked into the swine urine and detected with the same conditions to evaluate the specificity of the method.

Results and discussion

Characterizations of the hybrid nanoflowers

The characterizations of the BSA-AuNCs are shown in the ESM (Fig. S1), which are similar to those in previous reported [34]. In principle, the self-assembly of the hybrid nanoflowers included three stages: (1) Formation of primary crystals of calcium phosphate, and calcium(II) and protein formed complexes through the coordination interaction of amide groups and metal ion; (2) formation of large agglomerates of protein and primary crystals; and (3) complete formation of a branched flower-like structure [21]. The hybrid nanoflowers were fabricated by adding the organic components to $CaCl_2$ solution, namely, BSA-AuNCs and Clen-BSA. As shown in Table S1, the amount of protein in the mixed solution decreased from 0.89 to 0.01 mg after the synthesis of the nanoflowers, protein consumption rate was estimated as 100%, thereby demonstrating that nearly all of the Clen-BSA and BSA-AuNCs were loaded on the nanoflowers. The fluorescence intensity of the nanoflowers had a slight enhancement compared with BSA-AuNCs, it is probably because of aggregation induced emission [35]. The nanoflowers exhibit red fluorescence under the UV lamp (Fig. S2), and as shown in Fig. 1a, the excitation and emission wavelengths are the same as those of BSA-AuNCs (360 nm and 640 nm, respectively). The result of fluorescence confocal microscopy further demonstrates that BSA-AuNCs are successfully encapsulated in the nanoflowers (Fig. 1b). The SEM and TEM images show that the nanoflowers have a size of approximately 492 nm (Fig. 1c and d). Moreover, the energy dispersive X-Ray spectroscopy (EDS) spectrum also reveals $Ca_3(HPO_4)_2$ and BSA-AuNCs in the nanoflowers (Fig. S3).

To confirm that the Clen-BSA was also immobilized on the nanoflowers, MNPs-SA-Biotin-mAb capture probes were mixed with the fluorescent-hybrid nanoflowers for 15 min as experimental group, and the fluorescence intensity of supernatant was measured after magnetic separation. Moreover, three controls of mixture solutions (Control 1: fluorescent-hybrid nanoflowers and SA-MNPs, Control 2: fluorescent-hybrid nanoflowers and MNPs, Control 3: BSA-AuNCs and SA-MNPs) were set. Figure 2a shows that the fluorescence intensity of experimental group and Control 1 decreased significantly but that of Controls 2 and 3 did not change compared with the nanoflower solution. The nanoflowers performed severe, non-specifically adsorb SA-MNPs. The possible cause of the non-specific adsorption was the 3D structure and physical property of fluorescent-hybrid nanoflowers, which led to the adsorption of protein. The nonspecificity may be eliminated when the protein loading capacity of the nanoflowers approached saturation. BSA was commonly used as block reagent, the amount of BSA in fluorescent-hybrid nanoflower solution was optimized, and 2.0% (*w/v*) BSA solution was selected (Figs. S4a). Under the condition, Fig. 2b shows that the fluorescence intensity of supernatant for the experimental group altered significantly after magnetic separation. Additionally, the TEM images and dynamic light scattering results (Fig. S4) indicate that the diameter of the nanoflowers and MNPs-SA-Biotin-mAb conjugate was larger than that of MNPs-SA-Biotin-mAb, thereby manifesting that the fluorescent-hybrid nanoflowers successfully combined with MNPs-SA-Biotin-mAb. Consequently, the fluorescent-hybrid nanoflowers have sufficiently integrated the dual functions of fluorescence signal output and biological recognition.

Optimization parameters of the fluorometric immunoassay

A one-step method was used to develop the fluorometric immunoassay originally. However, the fluorescence of hybrid nanoflowers was seriously affected by the matrix effects of swine urine, resulting in irregular alteration of fluorescence (Table S2). Therefore, a two-step method was adopted, in which MNPs-SA-Biotin-mAb was used to isolate Clen from swine urine. Then, the nanoflowers were coupled with the remaining binding sites of MNPs-SA-Biotin-mAb. It suggests that the matrix effects were reduced dramatically after two immunomagnetic separation. Therefore, to obtain optimum performances of the method, the following parameters were optimized: (a) amount of SA-MNPs; (b) amount of biotinylated Clen-mAb; (c) incubation time. Respective data and figures are given in the ESM (Fig. S5). The following experimental conditions were found to give best results: (a) optimal amount of SA-MNPs: 50 μg; (b) optimal amount of biotinylated Clen-mAb: 10.2 μg; (c) best incubation time: 15 min.

Performances of the fluorometric immunoassay for Clen detection in samples

Different concentrations of Clen standard were spiked into the blank swine urine sample, and the final concentrations were

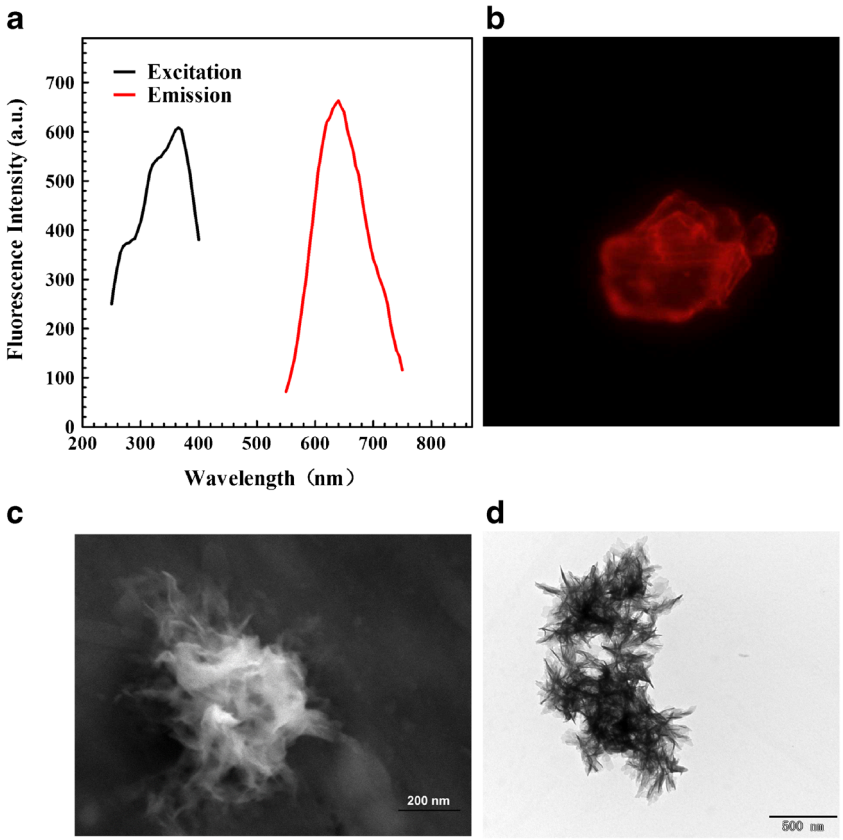

Fig. 1 Characterizations of hybrid nanoflowers with fluorescence spectrum (**a**), fluorescence confocal microscopy (**b**), SEM (**c**), and TEM (**d**)

0.5, 1.0, 2.0, 4.0, 8.0, 10.0, 20.0, 30.0, 40.0 μg L^{-1}. Under optimal conditions, the calibration plot was obtained by testing these standard solutions with the fluorometric immunoassay. Table S3 shows that the fluorescence intensity alteration (ΔF=F-F0, F and F0 represented the fluorescence intensity with and without Clen) increased with increasing concentration of Clen from 0 to 40.0 μg L^{-1}. The fluorescence intensity increased significantly from 15.05 ± 0.40 to 47.91 ± 0.39 (a.u.), and the corresponding ΔF value was 32.86 ± 0.33 (a.u.). The calibration plot was constructed by plotting the ΔF values against the logarithm of Clen concentrations in the samples (Fig. 3a). It exhibited a good linear range from 0.5 to 40.0 μg L^{-1} with a reliable correlation of coefficient (R^2 = 0.9936), the linear equation is y = 7.52 lg(x) + 5.10 (where y is the ΔF and x is Clen concentration). The limit of detection was calculated as low as 0.167 μg L^{-1} (3*σ/m = 3*0.419/7.52, where σ is the standard deviation of the blank and m is the slope of the calibration plot), which is much lower than the Codex Alimentarius Commission regulations residue limit [25]. A lot of methods have been developed for Clen detection, here, the performances of published assays have been summarized in Table 1, it suggests the fluorometric

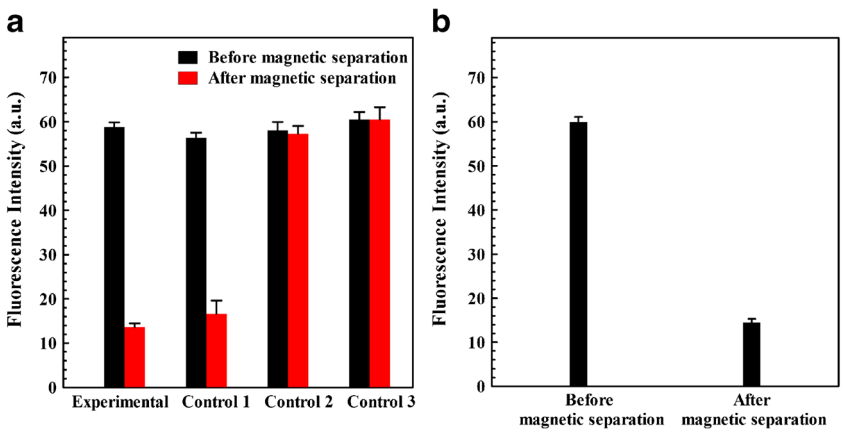

Fig. 2 Evaluation of the nonspecific adsorption of fluorescent-hybrid nanoflowers (**a**). Fluorescence intensity alteration with 2.0% BSA before and after immunomagnetic separation (**b**)

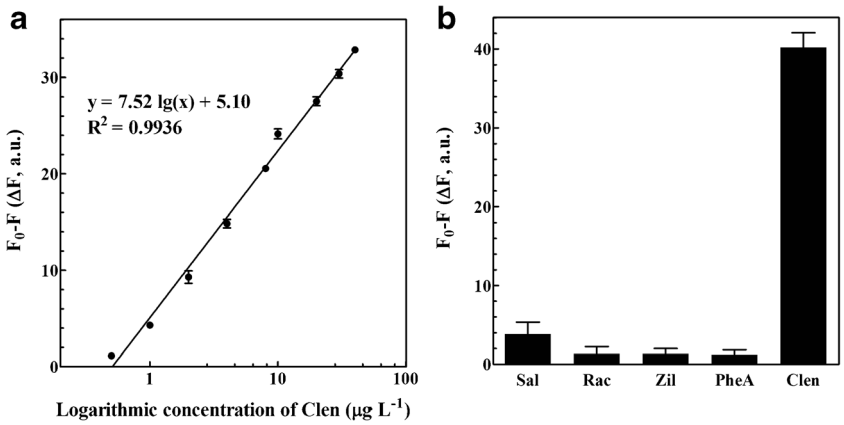

Fig. 3 Calibration plot for the detection of Clen with 0.5, 1.0, 2.0, 4.0, 8.0, 10.0, 20.0, 30.0, 40.0 μg L^{-1} (**a**) and the selectivity of the method (**b**). F and F0 represented the fluorescence intensity (measured at excitation/emission wavelengths of 360/640 nm) with and without Clen, respectively

immunoassay developed on the basis of nanoflowers and immunomagnetic separation is comparable to that of other methods for the detection of Clen residues. However, two immunomagnetic separations are needed because the nanoflowers were seriously affected by the matrix effects of samples, which is a limitation of the method. Further work will be done for overcome the drawback to develop a more simple and time-saving approach in our future work.

The selectivity of the method was evaluated by detecting the swine urine samples spiked with 50.0 μg L^{-1} of Clen, Sal, Rac, Zil, and PheA. The presence of Clen caused significant fluorescence intensity alteration, whereas spiking with Sal, Rac, Zil, and PheA has no effect (see Fig. 3b). The established approach is specific to Clen detection.

The accuracy of the fluorometric immunoassay was evaluated by analyzing three spiked swine urine samples with 0.5 μg L^{-1}, 5.0 μg L^{-1}, 10.0 μg L^{-1} of Clen concentrations. The intra-assay was finished within 1 day, and the inter-assay was completed every 3 days for 15 days continuously. Table 2 shows the average recoveries for the intra-assay were in the range of 92.7–109.1% with relative standard deviation in the range 3.95–5.46%. The results for inter-assay ranged from 101.2 to 125.7% and 3.89 to 11.6%. Thus, the results are acceptable levels of precision for the strategy detection of Clen in swine urine.

Validation of the method by LC-MS/MS with real samples

Five swine urine samples collected from Beijing City and Zhejiang Province were simultaneously tested by LC-MS/MS and the established fluorometric immunoassay, results of the two assays indicated that all of the five samples are free of Clen. Besides, to evaluate the acceptability of the method, the five blank swine urine samples were spiked with Clen standards and then tested by the two methods. The results are

Table 1 Comparison with the published methods for Clen detection

Methods	Materials used	Linear range	LOD (μg L^{-1})	Samples	References
Immunoassay	Fluorescent-hybrid nanoflowers	0.5–40 μg L^{-1}	0.167	Swine urine	This work
Quartz crystal microbalance sensor array	Molecular imprinted polymers	10^{-5}–0.01 mM	3.0	Swine urine	[25]
Surface-Enhanced Raman Spectroscopy	Graphene oxide/gold nanoparticle hybrids	0.5–20 μg L^{-1}	0.5	Animal urine	[32]
Colorimetric assay	Nanodiamonds and Gold nanoparticles	5.3–335.4 μg L^{-1}	0.166	Human urine	[36]
Lateral test strip	Gold nanoparticles	–	3.0	Swine urine	[37]
Fluorescence sensor	Palmatine-cucurbit[7]uril complex	11–4200 μg L^{-1}	4.0	Porcine muscle and swine urine	[38]
Paper-based microfluidic ELISA	Microfluidic paper-based analytical device	–	0.2	Water and milk	[39]

Table 2 Precision and accuracy of the fluorometric immunoassay in Clen spiked swine urine samples ($n = 3$)

Spiked level ($\mu g\ L^{-1}$)	Intra-assay		Inter-assay	
	Average recovery (%)	RSD (%)	Average recovery (%)	RSD (%)
0.5	109.1	5.46	125.7	5.86
5	94.7	4.36	110.2	11.6
10	92.7	3.95	101.2	3.89

shown in Fig. S6, which indicated that there is a favorable correlation ($R^2 = 0.954$) between the measured values of Clen tested by LC-MS/MS and the fluorometric immunoassay. Thus, it suggests that the fluorometric immunoassay exhibits potential in separating and detecting Clen residues in the real samples.

Conclusions

In summary, novel fluorescent-hybrid nanoflowers were fabricated, which made immobilization of BSA-AuNCs and Clen-BSA avoid the use of organic solvent and complex reaction. A fluorometric immunoassay based on the nanoflowers and immunomagnetic separation was successfully established, which is able to detect Clen residues in swine urine samples with satisfactory recoveries and acceptable accuracy. The flexible fabrication of hybrid nanoflowers has the potentials for preparing multiplex conjugations by immobilizing biomolecules (i.e., antigens and antibodies) with different fluorescent nanoclusters, and the multiplex conjugations will be beneficial for development of highthrough-put strategies for multiples targets detection in food security.

Acknowledgments This work was supported by the National Natural Science Foundation of China (31672600) and Sanming Project of Medicine in Shenzhen (SZSM201611068). And the authors appreciate the cooperation of other faculty members in the Department of Pharmacology and Toxicology of the College of Veterinary Medicine at China Agricultural University.

Compliance with ethical standards This article does not contain any studies with human participants or animals performed by any of the authors. The author(s) declare that they have no competing interests.

References

1. Masiá A, Suarez-Varela MM, Llopis-Gonzalez A, Picó Y (2016) Determination of pesticides and veterinary drug residues in food by liquid chromatography-mass spectrometry: a review. Anal Chim Acta 936:40–61
2. Wu D, Du D, Lin Y (2016) Recent progress on nanomaterial-based biosensors for veterinary drug residues in animal-derived food. TrAC Trend Anal Chem 83:95–101
3. Esteve-Turrillas FA, Abad-Fuentes A (2013) Applications of quantum dots as probes in immunosensing of small-sized analytes. Biosens Bioelectron 41:12–29
4. Deng SL, Shan S, Xu CL, Liu DF, Xiong YH, Wei H, Lai WH (2014) Sample preincubation strategy for sensitive and quantitative detection of clenbuterol in swine urine using a fluorescent microsphere-based immunochromatographic assay. J Food Prot 77(11):1998–2003
5. Shang L, Dong S, Nienhaus GU (2011) Ultra-small fluorescent metal nanoclusters: synthesis and biological applications. Nano Today 6(4):401–418
6. Zhang L, Wang E (2014) Metal nanoclusters: new fluorescent probes for sensors and bioimaging. Nano Today 9(1):132–157
7. Zheng Y, Lai L, Liu W, Jiang H, Wang X (2017) Recent advances in biomedical applications of fluorescent gold nanoclusters. Adv Colloid Interf Sci 242:1–16
8. Hu L, Deng L, Alsaiari S, Zhang D, Khashab NM (2014) "light-on" sensing of antioxidants using gold nanoclusters. Anal Chem 86(10): 4989–4994
9. Jiang H, Su X, Zhang Y, Zhou J, Fang D, Wang X (2016) Unexpected thiols triggering photoluminescent enhancement of cytidine stabilized au nanoclusters for sensitive assays of glutathione reductase and its inhibitors screening. Anal Chem 88(9):4766–4771
10. Li W, Chen B, Zhang H, Sun Y, Wang J, Zhang J, Fu Y (2015) BSA-stabilized Pt nanozyme for peroxidase mimetics and its application on colorimetric detection of mercury(II) ions. Biosens Bioelectron 66:251–258
11. Xu M, Gao Z, Wei Q, Chen G, Tang D (2016) Label-free hairpin DNA-scaffolded silver nanoclusters for fluorescent detection of Hg^{2+} using exonuclease(III)-assisted target recycling amplification. Biosens Bioelectron 79:411–415
12. Deng H, Zhang L, He S, Liu A, Li G, Lin X, Xia X, Chen W (2015) Methionine-directed fabrication of gold nanoclusters with yellow fluorescent emission for Cu^{2+} sensing. Biosens Bioelectron 65: 397–403
13. Xu Y, Zhang P, Wang Z, Lv S, Ding C (2018) Determination of the activity of telomerase in cancer cells by using BSA-protected gold nanoclusters as a fluorescent probe. Microchim Acta 185:198. https://doi.org/10.1007/s00604-018-2734-5
14. Lan J, Zou HY, Wang Q, Zeng P, Li YF, Huang CZ (2016) Sensitive and selective turn off-on fluorescence detection of heparin based on the energy transfer platform using the BSA-stabilized au nanoclusters/amino-functionalized graphene oxide hybrids. Talanta 161:482–488
15. Guo X, Wu F, Ni Y, Kokot S (2016) Synthesizing a nano-composite of BSA-capped au nanoclusters/graphitic carbon nitride nanosheets as a new fluorescent probe for dopamine detection. Anal Chim Acta 942:112–120
16. Martín-Barreiro A, De SM, Galbán J (2018) Gold nanoclusters as a quenchable fluorescent probe for sensing oxygen at high temperatures. Microchim Acta 185(3):171. https://doi.org/10.1007/s00604-018-2676-y
17. Yang S, Jiang Z, Chen Z, Tong L, Lu J, Wang J (2015) Bovine serum albumin-stabilized gold nanoclusters as a fluorescent probe for determination of ferrous ion in cerebrospinal fluids via the Fenton reaction. Microchim Acta 182(11–12):1911–1916
18. Wei T, Du D, Zhu M, Lin Y, Dai Z (2016) An improved ultrasensitive enzyme-linked immunosorbent assay using hydrangea-like antibody-enzyme-inorganic three-in-one nanocomposites. ACS Appl Mater Interfaces 8(10):6329–6335
19. Ye R, Zhu C, Song Y, Song J, Fu S, Lu Q, Yang X, Zhu M, Du D, Li H, Lin Y (2016) One-pot bioinspired synthesis of all-inclusive

protein-protein nanoflowers for point-of-care bioassay: detection of E. Coli O157:H7 from milk. Nanoscale 8(45):18980–18986
20. Cui J, Jia S (2017) Organic-inorganic hybrid nanoflowers: a novel host platform for immobilizing biomolecules. Coord Chem Rev 352:249–263
21. Ge J, Lei J, Zare RN (2012) Protein-inorganic hybrid nanoflowers. Nat Nanotechnol 7(7):428–432
22. Zhang Z, Zhang Y, Song R, Wang M, Yan F, He L, Feng X, Fang S, Zhao J, Zhang H (2015) Manganese(II) phosphate nanoflowers as electrochemical biosensors for the high-sensitivity detection of ractopamine. Sensors Actuators B Chem 211:310–317
23. Mann S (2009) Self-assembly and transformation of hybrid nano-objects and nanostructures under equilibrium and non-equilibrium conditions. Nat Mater 8(10):781–792
24. Liu Y, Chen J, Du M, Wang X, Ji X, He Z (2017) The preparation of dual-functional hybrid nanoflower and its application in the ultra-sensitive detection of disease-related biomarker. Biosens Bioelectron 92:68–73
25. Feng F, Zheng J, Qin P, Han T, Zhao D (2017) A novel quartz crystal microbalance sensor array based on molecular imprinted polymers for simultaneous detection of clenbuterol and its metabolites. Talanta 167:94–102
26. Yan F, Zhang Y, Zhang S, Zhao J, Liu S, He L, Feng X, Zhang H, Zhang Z (2015) Carboxyl-modified graphene for use in an immunoassay for the illegal feed additive clenbuterol using surface plasmon resonance and electrochemical impedance spectroscopy. Microchim Acta 182(3–4):855–862
27. Ji R, Chen S, Xu W, Qin Z, Qiu JF, Li CR (2018) A voltammetric immunosensor for clenbuterol based on the use of a MoS2-AuPt nanocomposite. Microchim Acta 185(4):209. https://doi.org/10.1007/s00604-018-2746-1
28. Zhang Z, Duan F, He L, Peng D, Yan F, Wang M, Zong W, Jia C (2016) Electrochemical clenbuterol immunosensor based on a gold electrode modified with zinc sulfide quantum dots and polyaniline. Microchim Acta 183(3):1089–1097
29. Peng T, Yang WC, Lai WH, Xiong YH, Wei H, Zhang JS (2014) Improvement of the stability of immunochromatographic assay for the quantitative detection of clenbuterol in swine urine. Anal Methods 6:7394–7398
30. Duan N, Gong W, Wu S, Wang Z (2017) Selection and application of ssDNA aptamers against clenbuterol hydrochloride based on ssDNA library immobilized SELEX. J Agric Food Chem 65(8):1771–1777
31. Jin X, Fang G, Pan M, Yang Y, Bai X, Wang S (2018) A molecularly imprinted electrochemiluminescence sensor based on upconversion nanoparticles enhanced by electrodeposited rGO for selective and ultrasensitive detection of clenbuterol. Biosens Bioelectron 102:357–364
32. Cheng J, Su X, Wang S, Zhao Y (2016) Highly sensitive detection of clenbuterol in animal urine using immunomagnetic bead treatment and surface-enhanced raman spectroscopy. Sci Rep UK 6:32637. https://doi.org/10.1038/srep32637
33. Shan S, Zhong Z, Lai W, Xiong Y, Cui X, Liu D (2014) Immunomagnetic nanobeads based on a streptavidin-biotin system for the highly efficient and specific separation of listeria monocytogenes. Food Control 45:138–142
34. Xie J, Zheng Y, Ying JY (2009) Protein-directed synthesis of highly fluorescent gold nanoclusters. J Am Chem Soc 131(3):888–889
35. Li D, Chen ZH, Mei XF (2017) Fluorescence enhancement for noble metal nanoclusters. Adv Colloid Interf Sci 250:25–39
36. Shellaiah M, Simon T, Venkatesan P, Sun KW, Ko F, Wu S (2018) Nanodiamonds conjugated to gold nanoparticles for colorimetric detection of clenbuterol and chromium(III) in urine. Microchim Acta 185(1):74. https://doi.org/10.1007/s00604-017-2611-7
37. Khaemba GW, Mukunzi D, Joel I, Guo LL, Suryobrobowo S, Song SS, Kuang H, Xu CL (2016) Development of monoclonal antibody and lateral test strip for sensitive detection of clenbuterol and related β_2-agonists in urine samples. Food Agriic Immunol 27(1):111–127
38. Jing X, Bai B, Zhang C, Wu W, Du L, Liu H, Yao G (2015) Rapid and sensitive determination of clenbuterol in porcine muscle and swine urine using a fluorescent probe. Spectrochim Acta A 136:714–718
39. Ma L, Nilghaz A, Choi JR, Liu X, Lu X (2018) Rapid detection of clenbuterol in milk using microfluidic paper-based ELISA. Food Chem 246:437–441